Oztoprak, S. & Bolton, M. D. (2013). *Géotechnique* **63**, No. 1, 54–70 [http://dx.doi.org/10.1680/geot.10.P.078]

Stiffness of sands through a laboratory test database

S. OZTOPRAK* and M. D. BOLTON†

Deformations of sandy soils around geotechnical structures generally involve strains in the range small (0·01%) to medium (0·5%). In this strain range the soil exhibits non-linear stress–strain behaviour, which should be incorporated in any deformation analysis. In order to capture the possible variability in the non-linear behaviour of various sands, a database was constructed including the secant shear modulus degradation curves of 454 tests from the literature. By obtaining a unique S-shaped curve of shear modulus degradation, a modified hyperbolic relationship was fitted. The three curve-fitting parameters are: an elastic threshold strain γ_e, up to which the elastic shear modulus is effectively constant at G_0; a reference strain γ_r, defined as the shear strain at which the secant modulus has reduced to $0{\cdot}5G_0$; and a curvature parameter a, which controls the rate of modulus reduction. The two characteristic strains γ_e and γ_r were found to vary with sand type (i.e. uniformity coefficient), soil state (i.e. void ratio, relative density) and mean effective stress. The new empirical expression for shear modulus reduction G/G_0 is shown to make predictions that are accurate within a factor of 1·13 for one standard deviation of random error, as determined from 3860 data points. The initial elastic shear modulus, G_0, should always be measured if possible, but a new empirical relation is shown to provide estimates within a factor of 1·6 for one standard deviation of random error, as determined from 379 tests. The new expressions for non-linear deformation are easy to apply in practice, and should be useful in the analysis of geotechnical structures under static loading.

KEYWORDS: laboratory tests; sands; statistical analysis; stiffness

INTRODUCTION

The degradation of shear modulus with strain has been observed in soil dynamics since the 1970s, and the dependence of secant shear modulus G on strain amplitude was illustrated for dynamic loading by a number of researchers using the resonant column test or improved triaxial tests (Seed & Idriss, 1970; Hardin & Drnevich, 1972a, 1972b; Iwasaki *et al.*, 1978; Kokusho, 1980; Tatsuoka & Shibuya, 1991; Yamashita & Toki, 1994). The same concept has been applied to static behaviour from the mid-1980s (Jardine *et al.*, 1986; Atkinson & Salfors, 1991; Simpson, 1992; Fahey & Carter, 1993; Mair, 1993; Jovicic & Coop, 1997). Today, non-linear soil behaviour is a widely known and well-understood concept. However, there are some limitations to incorporating this concept into numerical models for sands because of the potential complexity of constitutive models, the requirements of special testing (Atkinson, 2000), and, above all, the difficulty of obtaining undisturbed samples of sandy materials. In geotechnical practice, decision-making must usually be based on simple calculations using a few parameters that can be found easily from routine tests. Simple but effective models of non-linear soil behaviour should be developed to satisfy this demand. The possible errors arising from the use of simple models must then be quantified.

The stiffness of soils cannot be taken as constant when strains increase to the magnitudes generally encountered around geotechnical structures. The degradation of shear modulus with strain should therefore be incorporated into deformation analyses. There are numerous publications in the literature on the deformation behaviour of sands. Studies based on micromechanics seek to reveal the physical origins of behaviour in the non-linear elastic region. Although the following section reviews the shear modulus degradation of sandy soils only in the context of continuum mechanics, some micromechanical insights will emerge later when data are examined. And although the current trend is for determining the stiffness of sandy soils by in situ testing, the focus here will be on the use of laboratory data obtained from reconstituted and/or high-quality undisturbed samples and reported in the literature. The issue here will be the degree of uncertainty involved in the prediction of such sophisticated data using routine classification data.

A tremendous amount of work has been done to determine the very-small-strain shear modulus and its reduction with strain. Necessarily, only a few studies will be mentioned. Following the development of the resonant column test, Hardin & Black (1966) demonstrated the influence of void ratio (e) and mean effective stress (p') on the maximum (elastic) shear modulus, G_0, through an empirical equation of the form

$$G_0 = A \cdot F(e) \cdot (p')^m \tag{1}$$

where $F(e)$ is a function of void ratio, and A and m are material constants. Hardin & Black (1966) proposed $F(e) = (e_g - e)^2/(1 + e)$, where different values of e_g, A and m were proposed for sands of differing angularity. This basis has been much used in research and practice; today there is a general acceptance of taking m as 0·50, which happens to conform to Herzian theory for the pressure dependence of conical contacts (Goddard, 1990).

Later research has demonstrated that it is the mean effective stress acting in the plane of shear that controls shear modulus, rather than the mean effective stress in three dimensions (Roesler, 1979). Accordingly, in the tests on axially symmetric soil samples to be reported here, the controlling effective stress should be taken as

Manuscript received 5 August 2010; revised manuscript accepted 21 March 2012. Published online ahead of print 12 October 2012. Discussion on this paper closes on 1 June 2013, for further details see p. ii.

* Department of Civil Engineering, Istanbul University, Turkey; former visiting researcher at the University of Cambridge, UK.
† Schofield Centre, Department of Engineering, University of Cambridge, UK.

$s' = (\sigma'_1 + \sigma'_3)/2$ rather than $p' = (\sigma'_1 + \sigma'_2 + \sigma'_3)/3$. Nevertheless, it will be p' that will be used in the following, chiefly because that is what the original authors invariably quoted. Once recognised, of course, this constant arithmetical factor can easily be accounted for in plane-strain applications, for example.

Seed & Idriss (1970) published the first database of shear modulus degradation curves for sand, for the purpose of earthquake site response analysis. This S-shaped curve was obtained for 75 tests on a total of 30 sands, with a wide range of confining pressure, relative density and void ratio. Hardin & Drnevich (1972b), Iwasaki *et al.* (1978), Kokusho (1980) and the many others showed that equation (1) can be used to calculate a shear modulus for small to medium strains. They used the $G/F(e)$–p' relation to obtain strain-dependent parameters A and m, which generally exhibited the same trend: A tends to decrease and m tends to increase with strain. Index m is generally 0·5 from very small to small strains and then increases towards 1 for large strains. Jovicic & Coop (1997) showed that both A and m have S-shaped relations with the logarithm of strain.

A number of researchers have advocated that the grain size and uniformity of sands affects their stiffness. Iwasaki & Tatsuoka (1977) defined, as an additional multiplier in equation (1), a parameter B representing the influence of uniformity coefficient U_c, and fines content. Menq (2003) proposed an additional multiplier depending on U_c, and suggested that index m was also affected. Hardin & Kalinski (2005) introduced a diameter parameter $f(D)$ to calculate the maximum shear modulus for gravelly soils, but the dimensional nature of this particular factor is problematic.

The non-linear stress–strain behaviour of soils at small to medium strains is mostly represented by some form of hyperbolic stress–strain relationship. Hardin & Drnevich (1972b) proposed this relationship as

$$\left(\frac{G}{G_0}\right) = \frac{1}{1 + (\gamma/\gamma_r)} \tag{2}$$

where G is the secant shear modulus at any strain, G_0 or G_{max} is the elastic (maximum) shear modulus (e.g. G at $\gamma = 0{\cdot}0001\%$), and γ_r is the reference shear strain, which is defined by τ_{max}/G_0. The disadvantage of this approach is the difficulty in finding τ_{max}. The authors also indicated that this true hyperbolic relationship did not generally fit their data. They therefore used a distorted strain scale, which they called 'hyperbolic shear strain'.

Fahey & Carter (1993) reorganised the hyperbolic model so that modulus reduction became a function of shear strength mobilisation, as seen in equation (3). In addition to requiring τ_{max}, this also uses empirical parameters f and g. They showed some success fitting this three-parameter model to the data of a wide range of soils.

$$\left(\frac{G}{G_0}\right) = 1 - f\left(\frac{\tau}{\tau_{max}}\right)^g \tag{3}$$

Darendeli (2001) proposed a modified hyperbolic model based on testing of intact sand-gravel samples

$$\left(\frac{G}{G_0}\right) = \frac{1}{1 + (\gamma/\gamma_r)^a} \tag{4}$$

where a is called the curvature parameter, and γ_r is the reference strain value at which $G/G_0 = 0{\cdot}50$. This model uses only two parameters, and the reference strain provides an efficient normalisation of shear strain.

In order to comprehend the non-linear elastic behaviour of sands, and to produce a best-fit functional relationship, a new database has been constructed incorporating shear modulus degradation curves from the literature. This curve-fitting process has led to new interpretations and definitions that facilitate prediction of the shear modulus degradation of sands with strain, based on elementary soil classification data.

STIFFNESS DATABASE OF SANDY SOILS

Because of the difficulty of sampling, and the requirements of sophisticated element tests, most engineers prefer in situ testing to laboratory testing to determine the stiffness of sands. However, extensive laboratory stiffness data already exist for sandy soils, appearing in publications from the 1970s onwards, aimed at identifying the maximum shear modulus and the rate of shear modulus reduction with strain. Researchers have used both reconstituted specimens and high-quality undisturbed samples with equipment adapted to measure small-to-medium strains with good resolution.

In order to collect all available shear modulus degradation curves and data from static and dynamic tests, a wide trawl was done through the literature. More than 70 references were used, and more than 500 curves were digitised to create a database. Eventually 454 tests were selected from 65 references. The relationship between normalised shear modulus (G/G_0) and shear strain (γ) for the 454 selected tests is plotted in Fig. 1. The corresponding 65 references with selected information from the database are summarised in Table 1. As seen in Fig. 1, points from each published test are merged to create a curved but well-defined degradation zone. Three different procedures were used to generate these points.

(*a*) If a G–γ or G/G_0–γ curve was drawn using a solid line, three points were located within each tenfold strain interval starting from 10^{-6} strain.
(*b*) If G–γ or G/G_0–γ data comprised points with a number of less than 20, then all the points were selected.
(*c*) If the number of points was more than 20, a similar process was adopted as for solid lines.

The scatter of points seen outside the general degradation zone in Fig. 1 is very limited, and mainly in the very small strain range; these are usually single data points arising, presumably, from inadequate resolution of strain. However, 5% of the published tests were excluded entirely. For example, the paper of Iwasaki *et al.* (1978) included 36 tests, but only 35 of them were used; also Kokusho (1980) published 18 tests, but two of them were excluded. The excluded tests deviated strongly from the general trend. In some references, the excluded soils were thought to be cemented, but in others there was no obvious reason for the deviation. Leaking membranes or some other major but unrecognised experimental problem may have occurred. As can be seen from Fig. 2, the boundaries of the stiffness degradation zone, for those 95% of tests that have been included, are very clearly defined.

The database covers a wide variety of sandy soils, including dry, wet, saturated, reconstituted and undisturbed samples of clean sands, gravels, sands with fines and/or gravels, and gravels with sands and fines, representing 60 different materials (e.g. Toyoura sand, Ottawa sand, undisturbed Ishikari sand). The samples were prepared to investigate the effects of changing the void ratio, relative density, anisotropy, drainage conditions and confining pressure, and were tested under drained and/or undrained conditions in static and dynamic tests. The various parameters and soil state/test numbers are given for all references in Table 1. It is suggested that these two columns should be evaluated together; the number in parentheses in the last column repre-

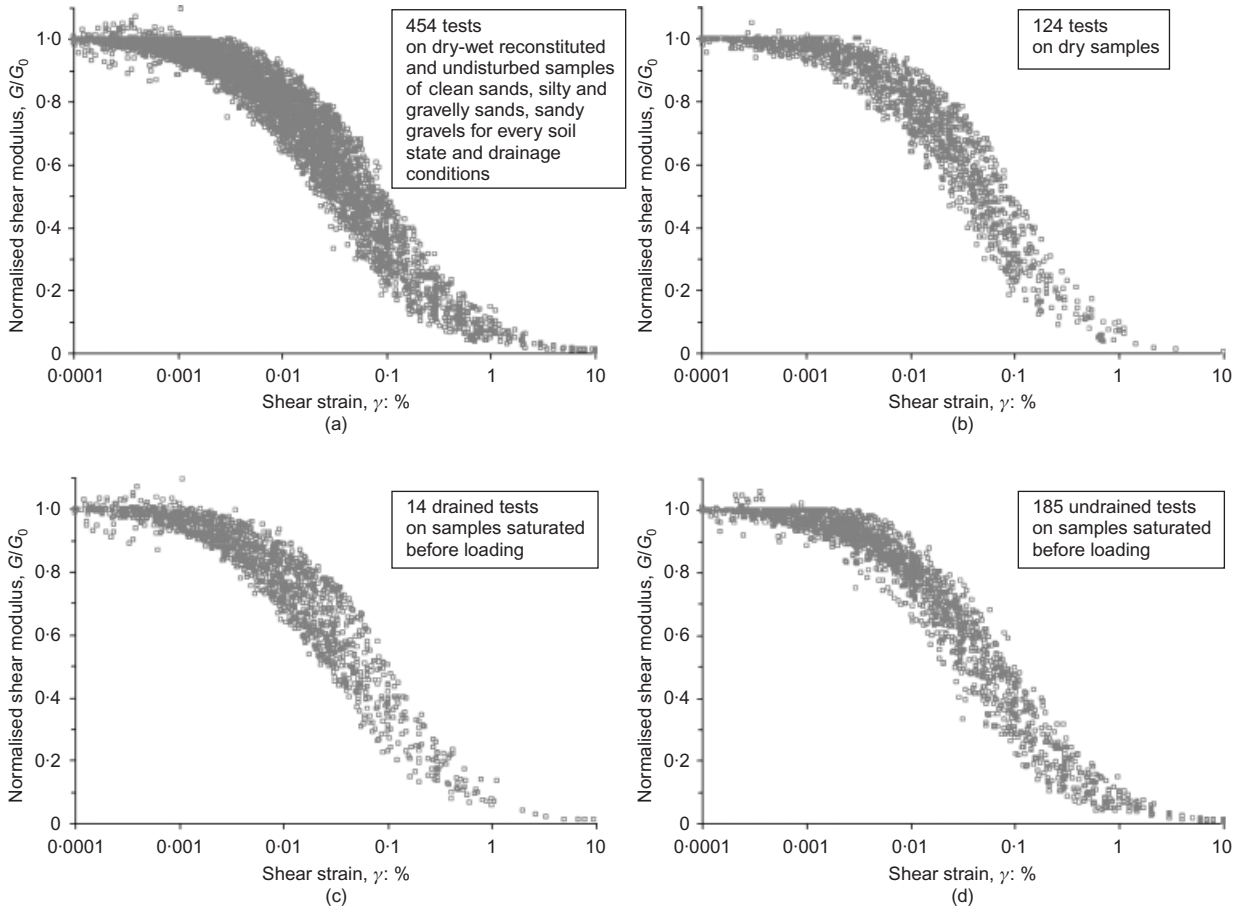

Fig. 1. Shear modulus degradation data from database

sents the number of sand states, and it is followed by the number of tests. For example, Chung *et al.* (1984) applied three different confining pressures on the same sample, so it is given as (1)3. In another row, Lo Presti *et al.* (1997) used six samples with different void ratios and tested them under the same confining pressure, so it is given as (6)6.

Since it includes so many references and test numbers, it is impractical to list all the details of the database. Fig. 3 was therefore prepared to illustrate the scope of the database. The materials are mostly sands of various gradings, but mainly quite uniform, with some gravels; the relative density is mostly high but with some looser samples; and the confining pressures are mostly between 50 and 600 kPa, with a median of 150 kPa. Caution must be exercised in using correlations based on the whole database to make predictions for other materials that have 'unusual' sets of parameter values that are sparsely represented in the database.

Dynamic test data are more common in the literature, and unavoidable for very small strains. The database accordingly includes a considerable number of cyclic tests. However, an attempt was made to limit the numbers of cycles in a test to about ten, up to which any effects are generally found to be negligible (Alarcon-Guzman *et al.*, 1989; Yasuda & Matsumoto, 1994). Larger numbers of cycles may affect the shear modulus degradation rate at medium to large strain levels, presumably because of the tendency of granular materials to compact during cyclic loading. This same tendency causes excess pore pressures to develop in undrained tests, which can ultimately lead to liquefaction. It is interesting to observe, therefore, that Fig. 1 demonstrates no obvious tendency for bias between tests on dry or damp sand and those on saturated sand, irrespective of whether they were conducted drained or undrained. This tends to confirm that volume change effects have been negligible in their influence on shear stiffness.

Other influences are also too subtle to make it worth extracting them. There are about ten samples whose OCR value is between 1 and 5. Regarding these data, the effect of OCR on the degradation curve is apparently very limited. Yamashita & Toki (1994) indicated that the shear modulus of sands at small strain levels is not affected by OCR, although a slight effect has been observed for medium strains. And, as Yamashita & Suzuki (1999) showed, whereas the direction of principal stress influences the elastic modulus G_0, it does not appear to change the $G/G_0{-}\gamma$ curve. Hence the normalised curve, given in Fig. 2, also allows for the effects of anisotropy.

MODELLING SHEAR MODULUS DEGRADATION

The best-fit functional relationship for the secant shear modulus degradation data of Fig. 1 is shown in Fig. 2 as a modified hyperbolic equation in the form

$$\left(\frac{G}{G_0}\right) = 1 \Big/ \left[1 + \left(\frac{\gamma - \gamma_e}{\gamma_r}\right)^a\right] \tag{5}$$

noting that for $\gamma < \gamma_e$, $G/G_0 = 1{\cdot}0$.

(*a*) Lower bound: $\gamma_e = 0$; $\gamma_r = 0{\cdot}02\%$; $a = 0{\cdot}88$.
(*b*) Mean: $\gamma_e = 0{\cdot}0007\%$; $\gamma_r = 0{\cdot}044\%$; $a = 0{\cdot}88$.
(*c*) Upper bound: $\gamma_e = 0{\cdot}003\%$; $\gamma_r = 0{\cdot}10\%$; $a = 0{\cdot}88$.

where G is the secant shear modulus at any strain; G_0 is the elastic (maximum) shear modulus (G at $\gamma = 0{\cdot}0001\%$); γ_r is the characteristic reference shear strain (shear strain at

Table 1. Summary of the database used for this study

Reference	Soil materials and description	Test type and drainage	Changed factors	Number of tests
Alarcon-Guzman *et al.* (1989)	Ottawa 20/30 sand (dry, vibrated)	RCT+TST, RCT	e, OCR, stress ratio, p'	(8)11
Arango (2006)	Calcareous and silica sands (dry, remoulded)	RCT	e, p'	(5)17
Cavallaro *et al.* (2003)	Noto soil (undisturbed lightly cemented silty sand)	RCT+CLTST (U)	e, p'	(2)2
Charif (1991)	Hostun sand (compacted)	TXT (D)	e, p'	(3)5
Chegini & Trenter (1996)	Glacial till (undisturbed, includes coarse material)	RCT (U)	PI, stone content, p'	(4)7
Chung *et al.* (1984)	Monterey sand No. 0	CLTXT (U)	p'	(1)3
Delfosse-Ribay *et al.* (2004)	Fontainebleau sand (with/without sodium silicate grouted)	RCT+CLTXT (U)	p'	(2)2
Dong *et al.* (1994)	Hime gravel (air-dried, compacted)	MLTXT (D)	e, D_{50}, U_c	(2)2
D'Onofrio & Penna (2003)	Silty sand (compacted)	RCT, CLTST (D)	e, p'	(4)7
Drnevich & Richart (1970)	Ottawa 30/50 sand (dry)	RCT	e, p'	(1)3
Ellis *et al.* (2000)	Fine and coarse silica sand (dry), Toyoura sand (dry and saturated)	RCT	e, D_{50}, U_c	(2)2
Fioravante *et al.* (1994)	Quiou sand (carbonatic, low-density reconstituted)	RCT (D)	e, OCR, p'	(5)7
Goto *et al.* (1987)	Gravel (undisturbed and reconstituted)	CLTXT (U)	I_D, p'	(2)2
Goto *et al.* (1992)	Gravel (undisturbed and reconstituted, 24% and 44% sand content)	CLTXT (U)	Sampling depth, G_o	(4)4
Hardin & Drnevich (1972a)	Sand (clean and dry)	CLSST	p'	(5)5
Hardin & Drnevich (1972b)	Sand (clean and dry)	CLSST	p'	(1)2
Hardin & Kalinski (2005)	Ottawa sand, sands (dry), gravel–sand–silt mixture (wet)	RCT (D)	e, p'	(2)6
Hashiba (1971)	Onahama sand (dry, remoulded)	SST	e, p'	(2)4
Hatanaka & Uchida (1995)	Tokyo gravel (undisturbed and reconstituted, sandy, includes fines)	CLTXT (U)	G_o	(2)2
Hatanaka *et al.* (1988)	Tokyo gravel (undisturbed and reconstituted, sandy, includes fines)	CLTXT (U)	p'	(2)4
Ishihara (1996)	Fujisawa sand (undisturbed and reconstituted)	TST (U)	e	(4)4
Ito *et al.* (1999)	Sandy gravel (undisturbed and improved by grouting)	CLTXT (D)	e, D_{50}, p'	(4)4
Iwasaki *et al.* (1978)	Toyoura, Ban-nosu, Iruma, Kinjo-1, Kinjo-2, Ohgi-Shima, Monterey sands	RCT, TST (D)	e, p'	(23)35
Jardine *et al.* (2001)	Dunqerque sand	TXT, TST (D)	OCR, test type	(2)3
Katayama *et al.* (1986)	Sand (undisturbed and reconstituted)	RCT	Sampling depth, G_o	(4)4
Koga *et al.* (1994)	Gravelly soil (dry, reconstituted)	CLTST	Gravel content	(5)5
Kokusho (1980)	Gifu and Toyoura sands (compacted, saturated)	CLTXT	Drainage, e, p'	(10)16
Kokusho & Esashi (1981)	Toyoura sand (saturated), undisturbed diluvial sand, gravel (saturated)	CLTXT (U)	e, p'	(3)11
Kokusho & Tanaka (1994)	Gravel (undisturbed and reconstituted)	CLTXT (U)	p'	(7)7
Laird & Stokoe (1993)	Sand (dry, remoulded)	CLTXT, RCT (U)	p'	(1)6
Lanzo *et al.* (1997)	Santa Monica and Antelope Valley sands (reconstituted, includes silt)	DSST (D)	e, OCR, p'	(6)10
Lo Presti *et al.* (1997)	Toyoura and Quiou sands (dry, hollow cylinder)	MLTST	e	(6)6
Maher *et al.* (1994)	Ottawa sand (medium and loose, untreated and chemically grouted)	RCT + CLTXT	I_D, concentration, curing time	(8)11
Menq (2003)	Washed mortar sand, sand and gravelly sand (dry)	RCT	e, D_{50}, U_c	(7)7
Menq & Stokoe (2003)	Sand (dense and dry)	RCT	p'	(1)3
Ogata & Yasuda (1982)	Gravelly soil (undisturbed, includes fines)	TXT	p'	(1)2
Park (1993)	Toyoura sand (air-dried, isotropic consolidated)	PSCT, TXT	OCR, p'	(2)2
Porovic & Jardine (1994)	Ham River sand (K_0 and isotropic consolidated)	RCT+TST (U)	Consolidation pressure, e, OCR	(8)8
Rollins *et al.* (1998)	Sand and gravelly sand (compacted, saturated)	RCT (U)	e, gravel content, p'	(1)5
Saxena *et al.* (1988)	Monterey sand (compacted, saturated, with/without cement, curing)	RCT (D)	I_D, cement content, curing time, p'	(14)22
Seed *et al.* (1986)	Gravel (Oroville and Pyramid materials)	CLTXT (U)	e	(2)2
Shibuya *et al.* (1996)	Higashi-Ohgijima sand (undisturbed)	CLTXT, TST (U)	Sampling depth, p'	(8)8
Silver & Seed (1971)	Quartz sand (crystal silica No. 20, dry)	CLSST	p'	(1)3
Stokoe *et al.* (1994)	Sand (undisturbed and dry-remoulded)	CLTST, RCT	e, p'	(5)9
Stokoe *et al.* (1999)	Silty sand (undisturbed)	RCT	Sampling depth, p'	(4)4
Tanaka *et al.* (1987)	Gravelly sand	CLTXT	Gravel content, p'	(2)6
Teachavorasinskun *et al.* (1991)	Toyoura sand (dense)	TSST (D)	e, OCR	(2)2

Teachavorasinskun *et al.* (1992)	Toyoura sand (remoulded, loose and dense, saturated)	CLTXT	*e*, drainage	(6)6
Tika *et al.* (1999)	Sand and sandy silt (remoulded; wet tamping)	RCT (U)	e	(2)2
Tika *et al.* (2003)	Sand (clean, with fines and gravel, air-pluviated and saturated)	RCT (D)	e, D_{50}, U_c, p'	(8)16
Tokimatsu & Hosaka (1986)	Nigata sand (undisturbed)	TXT (U)	D_{50}, U_c	(2)2
Tokimatsu *et al.* (1986)	Sand (undisturbed and reconstituted)	CLTXT (U)	G_0, p'	(2)2
Vinale *et al.* (1999)	Metramo silty sand (wet compacted, consolidated)	RCT (U)	Consolidation pressure, e, w	(9)9
Yamashita & Suzuki (1999)	Toyoura sand (remoulded, isotropically or anisotropically consolidated)	RCT	Consolidation condition, drainage	(8)14
Yamashita & Toki (1994)	Ishikari and Soma sands (undisturbed and reconstituted)	CLTXT, CLTST	Drainage, G_0, p'	(10)25
Yamashita *et al.* (1997)	Higashi-Ohgishima sand (undisturbed and reconstituted)	CLTXT (U)	e, D_{50}, U_c, p'	(18)21
Yang (2007)	Ottawa 20/30 and Monterey 0/30 sands (remoulded)	RCT	e, p'	(2)4
Yasuda (1992)	Gravel (undisturbed sample from Miho Dam, well graded)	CLTXT (D)	p'	(1)4
Yasuda & Matsumoto (1993)	Toyoura sand, gravel (air-dried, compacted, consolidated)	CLTSST (D)	p'	(4)16
Yasuda & Matsumoto (1994)	Gravel (compacted and consolidated, well graded)	CLTXT (D)	e, D_{50}, U_c, p'	(3)8
Yasuda *et al.* (1996)	Gravel (undisturbed and reconstituted, loading and unloading during test)	MLTXT, CLTXT	p'	(9)15

CL, cyclic loading; ML, monotonic loading; RCT, resonant column test; TXT, triaxial test; TST, torsional shear test; SST, simple shear test; TSST, torsional simple shear test.

Fig. 2. (a) Fitting a hyperbola to the data; (b) curve-fitting parameters

$G/G_0 = 0{\cdot}50$); a is the curvature parameter; and γ_e is the elastic threshold strain beyond which the shear modulus falls below its maximum. This equation is in the form proposed by Darendeli (2001), but including γ_e as an additional curve-fitting parameter, which enables the expression to cover cementation and interlocking effects at small strains, as also influenced by changes in the confining pressure.

If, on the other hand, the original relation for strain-dependent shear modulus given as equation (1) is formulated as a dimensionless equation, then it can be written

$$G = \frac{A(\gamma) \cdot p_a}{(1+e)^3} \cdot \left(\frac{p'}{p_a}\right)^{m(\gamma)} \tag{6}$$

where $A(\gamma)$ and $m(\gamma)$ are strain-dependent parameters, and p_a is a reference pressure of 100 kPa (effectively, the atmospheric pressure). Here, the simpler void ratio function $1/(1+e)^3$ was preferred to that of Hardin & Black (1966), following statistical checks to demonstrate that the effects were imperceptible or slightly beneficial in reducing scatter.

Normalisation of strain using the reference strain γ_r in equation (5) provides the most effective way of representing shear modulus degradation, but equation (6) provides the best understanding of other parametric influences on G. The use of equations (5) and (6) in sequence can provide a method for refining optimum functional relationships.

With the available information on p' and e from the database, log-log graphs of $G(1+e)^3/p_a$ against p'/p_a are shown in Fig. 4, where the strain-dependent parameters $A(\gamma)$ and $m(\gamma)$ are deduced for various strains. Despite the scatter, the trends are consistent with the literature. In principle, of course, the A and m coefficients may also be a function of

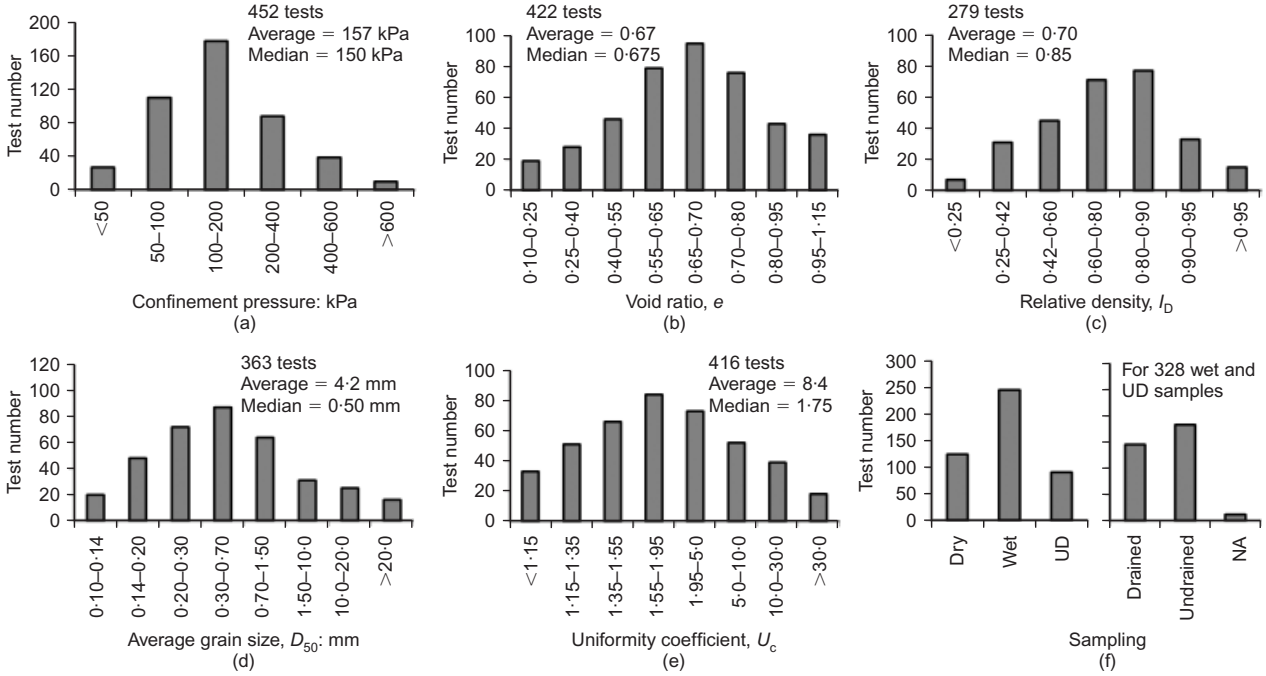

Fig. 3. Statistical information about database in terms of test numbers

p'. In order to investigate this, equations (5) and (6), which are alternative methods of representing shear modulus calculations at any strain level, can be compared.

To plot the results of equation (6) on the mean curve of G/G_0 against γ, p' in equation (6) can be assigned as 150 kPa, which is the average value of the median stress range in Fig. 3. Since G/G_0 is to be calculated, the void ratio function cancels, and is not required. Using p', $A(\gamma)$ and $m(\gamma)$ from Fig. 4, the G/G_0 values can readily be calculated and placed on Fig. 5(a), where they lie very close to the mean curve, but not exactly on it. Since the normalised shear modulus curve gives a more reliable relation than the scattered relationship shown in Fig. 4, it is preferred to modify the $A(\gamma)$ and $m(\gamma)$ values slightly from the values listed in Fig. 4 so as to fit exactly the mean curve in Fig. 5(a). The refined values appear in Fig. 6.

Once the calculated G/G_0 values of equation (5) have been fitted to the mean hyperbolic curve in Fig. 5(a) for the mean pressure $p' = 150$ kPa, other p' values can be inserted in equation (6), and appropriate values of γ_e and γ_r can be derived from equation (5) to fit the new curves. The resulting family of degradation curves for varying p' is shown in Fig. 5(b). Fig. 6(b), accumulating the results of 379 tests, shows that G_0 can best be expressed as a function of $(p')^{0.5}$ at very small strains and as a function of p' for large strains. If the resulting $m(\gamma)$ relation is compared with the published

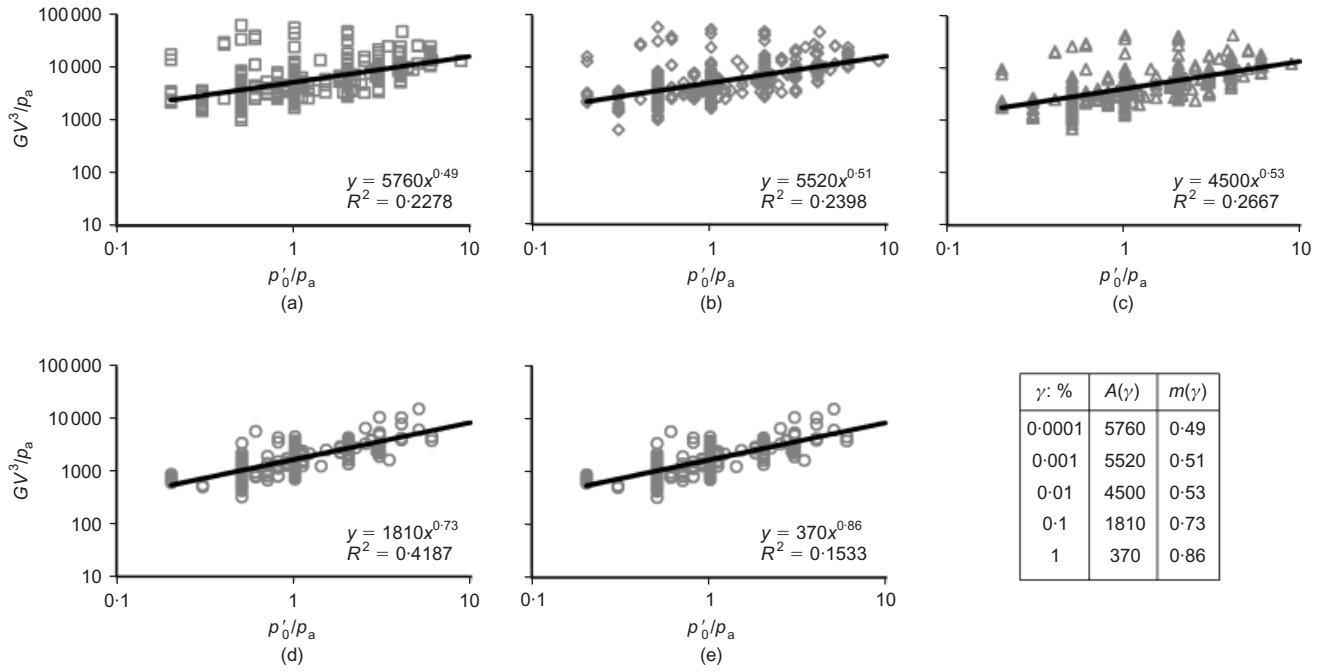

γ: %	$A(\gamma)$	$m(\gamma)$
0·0001	5760	0·49
0·001	5520	0·51
0·01	4500	0·53
0·1	1810	0·73
1	370	0·86

Fig. 4. Shear modulus variation with mean effective stress: (a) $\gamma = 0{\cdot}0001\%$ (379 tests); (b) $\gamma = 0{\cdot}001\%$ (379 tests); (c) $\gamma = 0{\cdot}01\%$ (374 tests); (d) $\gamma = 0{\cdot}1\%$ (221 tests); (e) $\gamma = 1\%$ (77 tests)

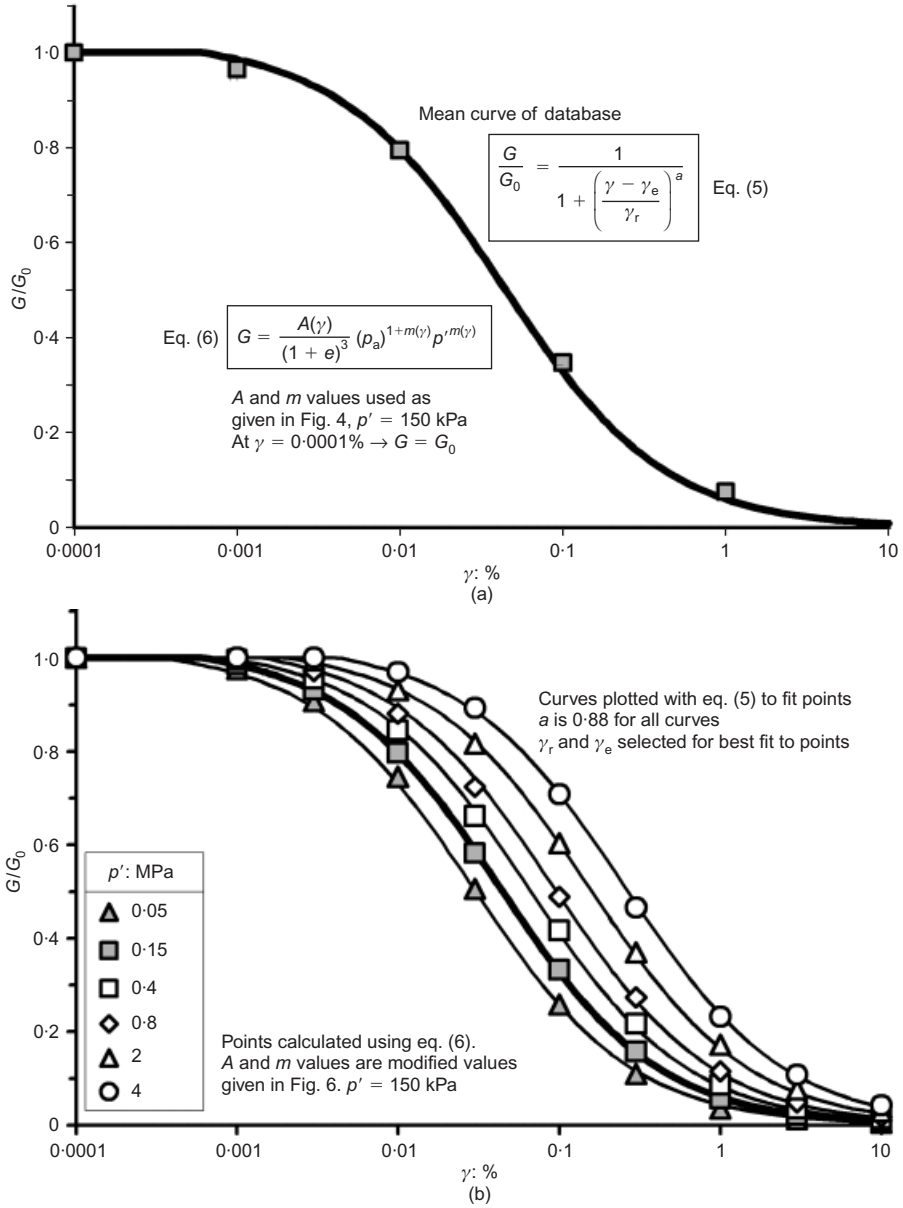

Fig. 5. Calibration of $m(\gamma)$ and $A(\gamma)$ parameters using equation (6) (symbols) with equation (5) (curves)

data of other researchers, as shown in Fig. 7, it now creates a trend line appropriate to most sands, verifying the modification process explained above.

Reference strain and elastic threshold strain

According to the database curve in Fig. 2, G/G_0 is 0·5 at a shear strain between 0·02% and 0·1%, with a mean of 0·044%. Using a constant value $a = 0{\cdot}88$ in equation (5), and changing the confining pressure progressively from 10 kPa to 4 MPa, leads to the interesting offsetting of the modulus degradation curves towards higher values of strain, as seen in Fig. 5(b). The trend of γ_e and γ_r increasing with confining stress is shown in normalised form in Fig. 8. Both γ_e and γ_r exhibit a logarithmic function with stress in the low-stress range ($p' < 70$ kPa). In the intermediate stress range (70 kPa $< p' <$ 600 kPa) the relation is nearly linear, but the rate of increase reduces slightly at even higher stresses. It must be presumed that grain contact deformation and damage are responsible for increasing characteristic strains in this way. For the most common confining stresses (70 kPa to 600 kPa), the sands typical of this database produce regressions for γ_e and γ_r as follows.

$$\gamma_e\ (\%) = (8 \times 10^{-5})\left(\frac{p'}{p_a}\right) + 6 \times 10^{-4} \tag{7}$$

$$\gamma_r\ (\%) = 0{\cdot}008\left(\frac{p'}{p_a}\right) + 0{\cdot}032 \tag{8}$$

Darendeli (2001) and Menq (2003) suggested a power relation between γ_r and p'. However, they both indicated that this relation tends to become linear for higher stresses. Menq (2003) also introduced the effect of uniformity coefficient for sands and gravels, and proposed an equation as follows.

$$\gamma_r = 0{\cdot}12U_c^{-0{\cdot}6}\left(\frac{p'}{p_a}\right)^{0{\cdot}5U_c^{-0{\cdot}15}} \tag{9}$$

Unlike the approaches of Darendeli (2001) and Menq (2003), it is considered convenient here to define the stress level as low, medium and high, and to accept a linear

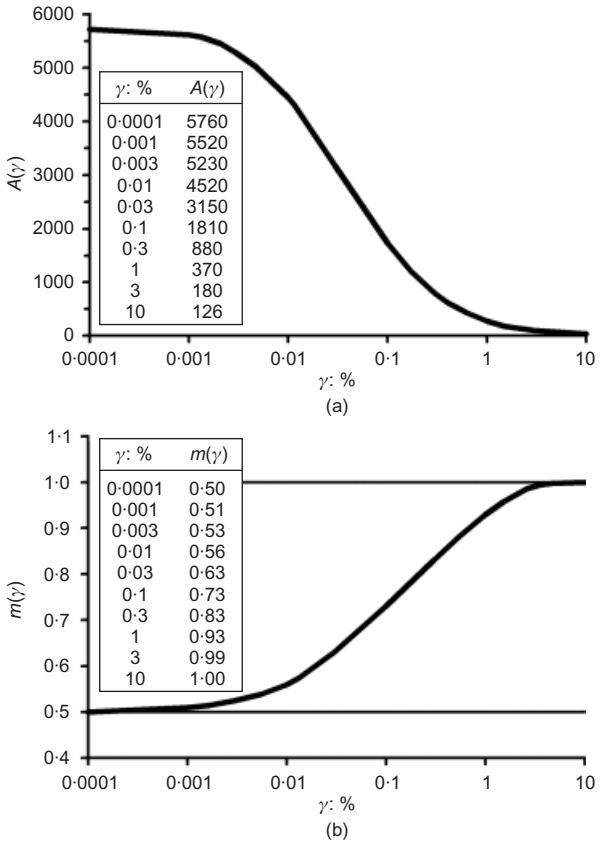

Fig. 6. Modified relations of $m(\gamma)$ and $A(\gamma)$

relation for medium and high stress levels. Moreover, a linear relation offers a better fit to the data than a power relation, at least for medium stress levels (70–600 kPa). Further support for a linear relation between γ_r and p' comes from the normalised shear modulus degradation of Toyoura sand reported by Iwasaki *et al.* (1978) and Kokusho (1980), and plotted in Fig. 9. The corresponding changes in γ_r are plotted in Fig. 10 for the stress range 50–300 kPa; the trend is obviously linear. The presumed cause of the different intercepts in Fig. 10 is the relative density of the respective trials, and possibly the influence of water at the smallest confining stresses. However, the gradients for this material in Fig. 10 are identical.

To generalise the relation between γ_r and p', the database was searched for all those soils on which tests were conducted at three or more confining pressures, providing data for the evolution of γ_r. This identified 24 sandy soils, and their data were split into four groups, as shown in Fig. 11. It can be confirmed that almost all the plots of γ_r exhibit a linear trend with increasing mean effective stress. As seen from Fig. 11, both uniformity and relative density exert a significant influence on the γ_r–p'/p_a relation. Fig. 11 therefore represents the functional dependence of γ_r on p', I_D and U_c for different states and types of sandy soils.

Various regressions are given in Fig. 12. Fig. 12(a) shows a power relation between γ_r and void ratio e, albeit with a moderate coefficient of determination $R^2 = 0{\cdot}54$. Fig. 12(b) shows negligible correlation between γ_r and relative density I_D, but Fig. 12(c) demonstrates a much-improved $R^2 = 0{\cdot}74$ for a power law correlation between γ_r and the product eI_D. This was initially unexpected. However, it is proposed that the group eI_D may be a surrogate for grain shape, which is the most significant omission from the current study of sand characteristics in relation to stiffness degradation. High void ratio for a rounded sand would indicate low relative density, so the product eI_D would also be small, whereas an angular sand could have a high void ratio at a high relative density and give a large product eI_D. So the magnitude of eI_D may indicate angularity. This possible explanation cannot be verified, since the authors whose work we have used did not generally remark on grain shape. Nevertheless, the statistical finding is significant.

If one equation will cover all these effects for calculating γ_r, it must be expressed in the form

$$\gamma_r\,(\%) = c\left(\frac{p'}{p_a}\right) + d \tag{10}$$

for medium stress levels. From Fig. 11, it is understood that U_c affects the slope of the γ_r–p'/p_a relation, and from Figs 10, 11 and 12 that the product eI_D affects the ordinate. Accepting these functional relationships, a multivariable regression analysis for medium stress levels then produced the relation

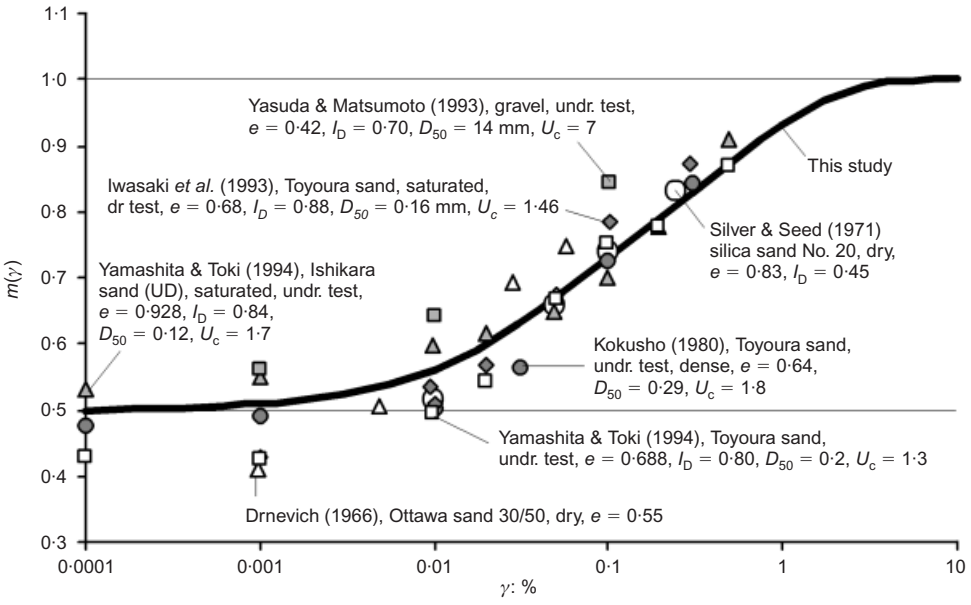

Fig. 7. Comparison of strain-dependent values of m with those from other work

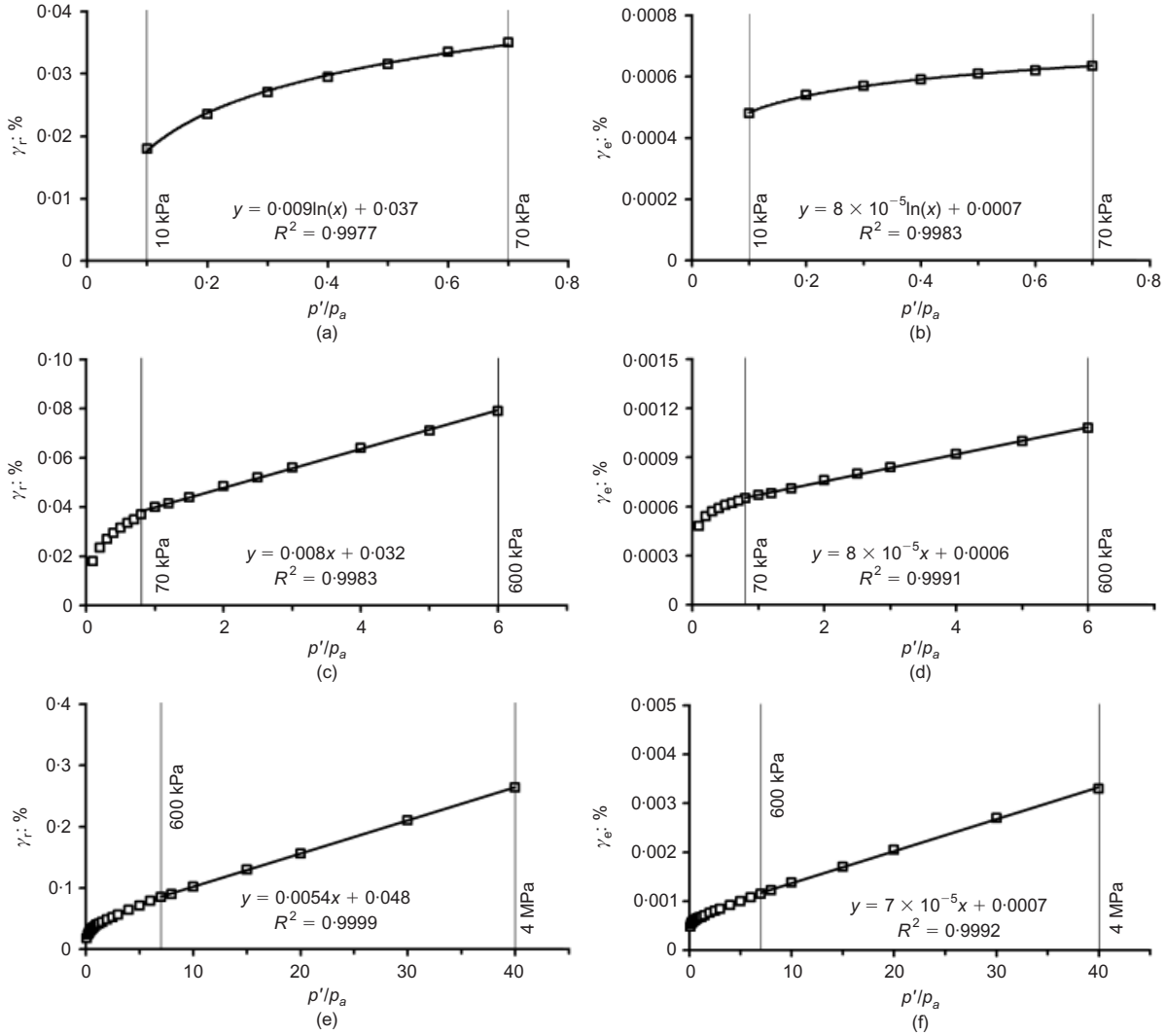

Fig. 8. Trend for evolution of γ_e and γ_r for different confining pressure ranges, derived from Fig. 5(b)

$$\gamma_r\,(\%) = 0{\cdot}01\,U_c^{-0{\cdot}3}\left(\frac{p'}{p_a}\right) + 0{\cdot}08eI_D \tag{11}$$

It is interesting to reflect on the physical origins of granular behaviour that could lead to the parametric influences in equation (11). An increase in uniformity coefficient U_c leads to a reduction in γ_r – that is, to a swifter loss of elastic stiffness with strain. McDowell & Bolton (1999) discussed the consequences of a dispersion of particle sizes in terms of the strain incompatibility between the fine matrix and the larger particle. The introduction of large particles inevitably causes premature sliding of smaller particles in contact with them. Since a sliding contact no longer contributes its tangential shear stiffness to the global shear modulus, the onset of sliding coincides with the reduction of G/G_0. In other words, the reference strain γ_r is reduced when there is a greater disparity in grain sizes. Equation (11) supports this finding.

According to equation (11), it must also be accepted that increased mean effective stress p' or increased relative density I_D (noting that an increase in I_D overwhelms the concomitant reduction in e) tends to protect the granular material somewhat from the reduction of stiffness due to strain: γ_r increases. This might be attributed in both cases to increased interlocking. Increased p' will lead to increased contact flattening, and a tendency to suppress degrees of freedom associated with sliding. Increasing I_D also wedges more grains in place. In these cases, small strains are more likely to involve elastic contact deformation mediated by a greater amount of grain rotation, and a reduced proportion of contact sliding. It may therefore be concluded that equation (11) is in accordance with a micromechanical understanding of soil behaviour.

Elastic threshold strain marks the onset of non-linearity, and is therefore associated with the onset of contact sliding. Identical micromechanical considerations apply to γ_e as to γ_r; it must therefore be anticipated that they will be correlated. The value of γ_e can be extracted from the database using the best-fit modulus reduction curve as expressed by equation (5). Furthermore, it is clear in Fig. 5(b) that γ_e increases at $G/G_0 = 1$ during an increase in the mean effective stress, and that it has the same trend as γ_r, albeit at a much smaller strain magnitude: this was set out in Fig. 8. Fig. 13 demonstrates that a simple linear relation can be derived between γ_e and γ_r (expressed in percentages) using all the available data, as

$$\gamma_e = 0{\cdot}0002 + 0{\cdot}012\gamma_r \tag{12}$$

Curvature parameter

The curvature parameter a varies from 0·75 to 1·0 in the database, and 0·88 is the average value for uncemented sands, as employed in equation (5). Darendeli (2001) suggested a constant value of 0·92 for a smaller range of

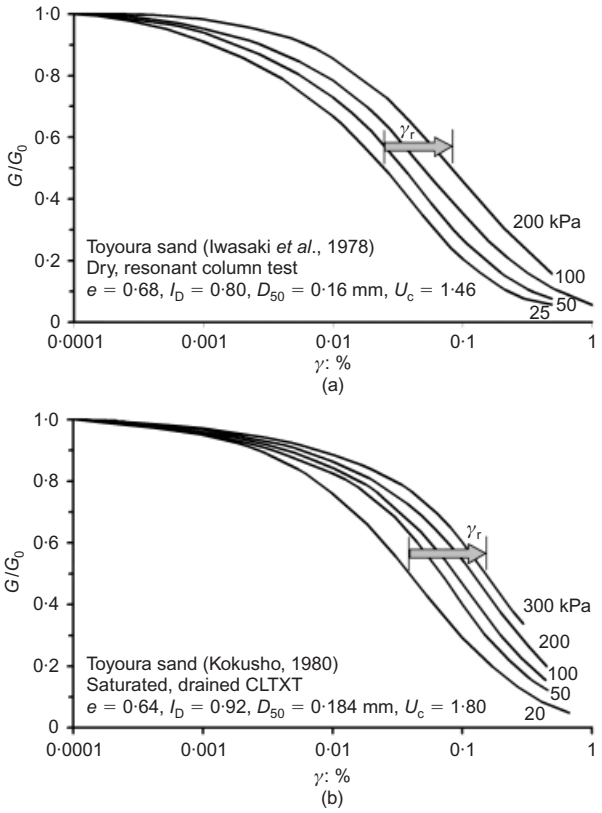

Fig. 9. Normalised shear modulus degradation curves of Toyoura sand shifting with mean effective stress

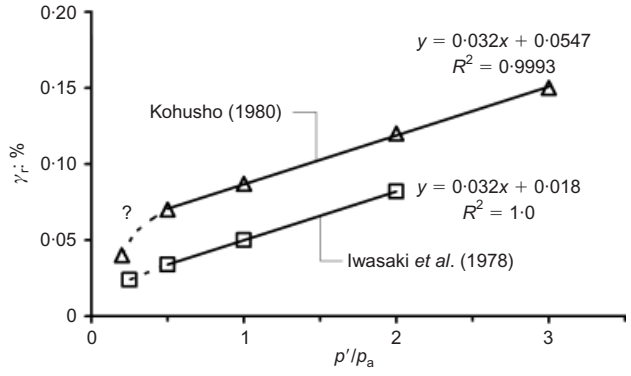

Fig. 10. Evolution of γ_r for Toyoura sand at increasing p'

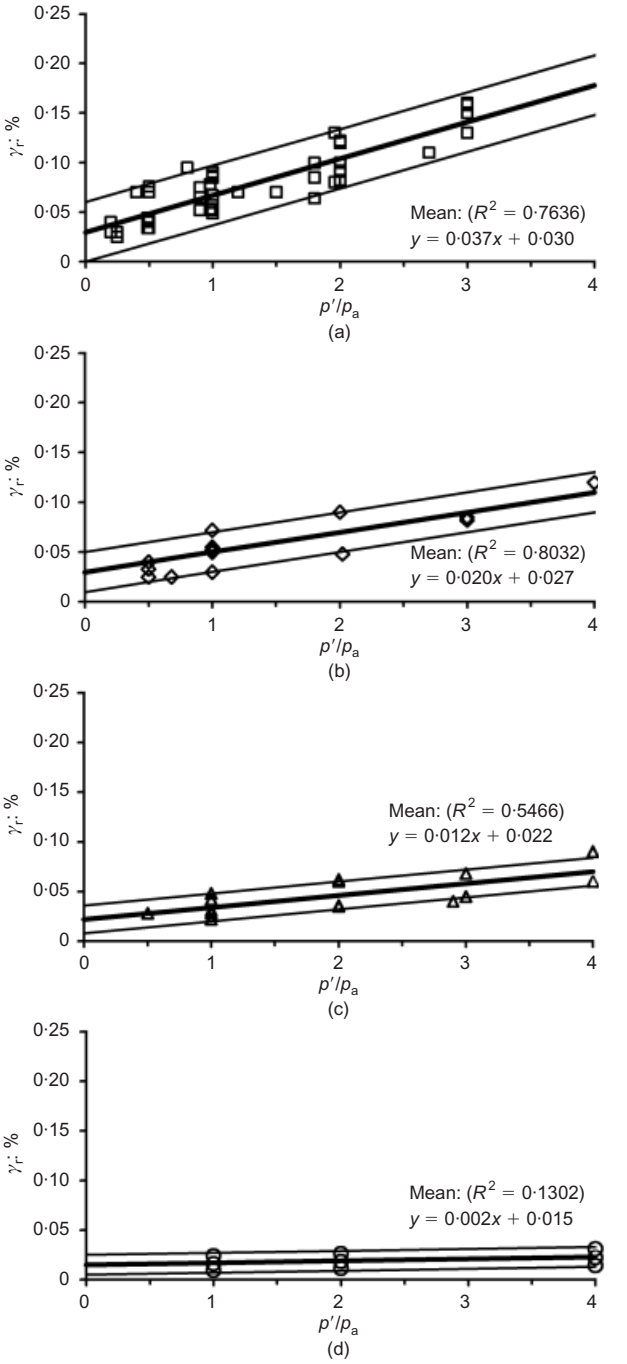

Fig. 11. Influence on γ_r of p' and soil type: (a) uniform sands, dense-medium ($U_c < 1{\cdot}8$, $I_D > 0{\cdot}60$, $e = 0{\cdot}64–0{\cdot}93$); (b) uniform sands, medium-loose ($U_c < 1{\cdot}8$, $I_D > 0{\cdot}60$, $e = 0{\cdot}58–1{\cdot}0$); (c) gravelly sands and sandy gravels ($6 > U_c > 70$, $I_D > 0{\cdot}40$, $e = 0{\cdot}25–0{\cdot}69$); (d) gravels, sandy gravels ($14 > U_c > 133$, $I_D > 0{\cdot}70$, $e = 0{\cdot}2–0{\cdot}3$)

undisturbed sandy and gravelly soils. According to Menq (2003), although the a value for Toyoura sand did not show any trend with confining pressure, the author's dry sandy and gravelly soils gave a trend in the form of $a = 0{\cdot}86 + 0{\cdot}1\log(p'/p_a)$. Nevertheless, according to the expanded database presented here, no clear evidence is seen of a dependence of a on mean effective stress. However, as shown in Fig. 14, a does appear to depend on soil type or condition, with reasonable correlations with void ratio, mean grain size and uniformity coefficient. It was found that multivariable regression was not required to express these variations, however. The best correlation ($R^2 = 0{\cdot}87$) was between curvature parameter a and uniformity coefficient U_c, as shown in Fig. 14(c).

$$a = U_c^{-0{\cdot}075} \tag{13}$$

Since an increase in U_c inevitably causes a reduction in void ratio e due to improved packing, the correlation (albeit weaker) between a and e in Fig. 14(a) is easily explained. Furthermore, the database shows that high U_c values were generally achieved by adding gravel to sand mixtures, thereby explaining the correlation (again, weaker) between a and D_{50}. Finally, it must be acknowledged that the micromechanical interpretation of equation (13) itself is that, once contact sliding has begun and G/G_0 has begun to reduce, uniformly graded soils ($U_c = 1$; $a = 1$) show a faster deterioration with strain than well-graded soils (e.g. $U_c = 10$; $a = 0{\cdot}85$), since a is a power in the denominator of equation (5). This interesting observation could be studied further using discrete-element modelling.

Whereas $a = 0{\cdot}88$ was used as the mean curvature param-

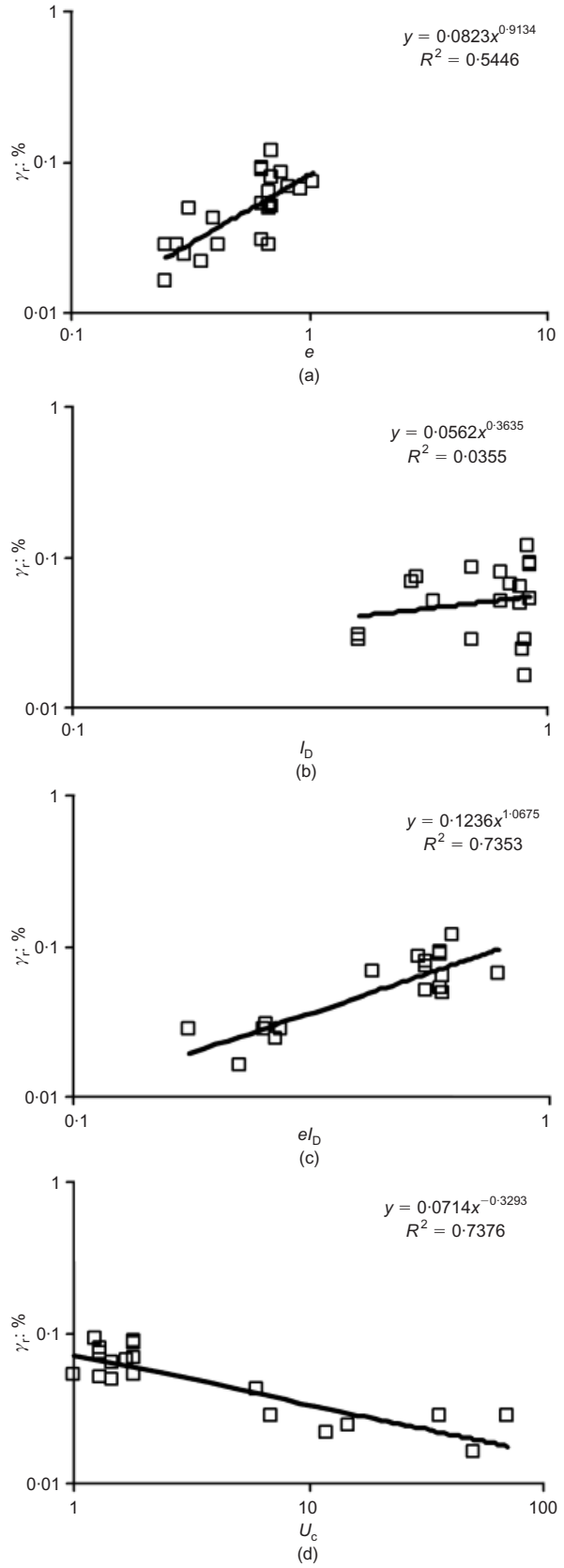

Fig. 12. Influence on γ_r of void ratio e, relative density I_D and uniformity coefficient U_c

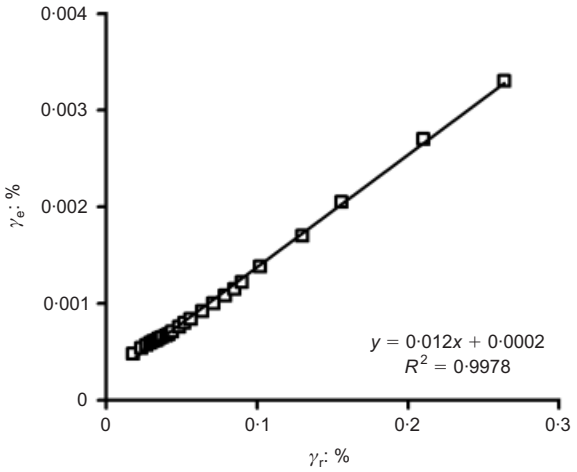

Fig. 13. Relation between γ_r and γ_e

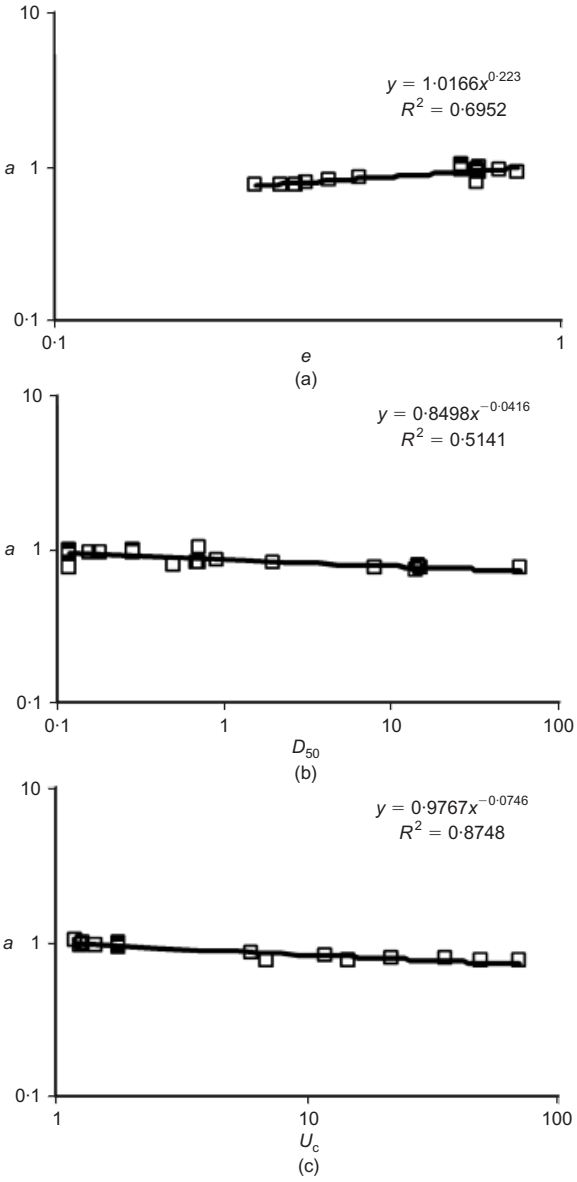

Fig. 14. Influence on curvature parameter a of void ratio and uniformity coefficient

eter for the $G/G_0-\gamma$ curves of the whole database of sandy soils in Fig. 2, the statistical analysis of variations between the characteristics of the soils and their test conditions has resulted in the more refined expression in equation (13). Although parameters such as γ_r and a may not appear to vary very much, their influence on soil stress–strain curves is by no means insignificant. Fig. 15(a) translates from G against γ at mean effective stress $p' = 100$ kPa into shear stress τ against γ in a hypothetical simple shear test. The

elastic stiffness at very small strains is taken as a constant $G_0 = 250$ MPa. In Fig. 15(a) it is shown that, for a typical sand with $a = 0{\cdot}88$, the influence of reference strain γ_r in the range 0·02–0·1% creates a fourfold variation in the mobilisation of shear stress up to 1% shear strain. Fig. 15(b) shows a more modest, but nevertheless significant, variation in expected mobilised shear stress due to variations of a within the typical range 0·80–1·0, for the average value of $\gamma_r = 0{\cdot}044\%$.

VALIDATION

In the case of unavailability of the linear elastic shear modulus value and its reduction by straining for a sandy soil, it is possible to calculate them with equations (5), (11), (12) and (13) proposed in this paper. Comparisons between measured and predicted values can be validated against the database. In Fig. 16(a) it is shown that 86% of the 345 calculated values of G_0 lie within a factor of 2 of the measured values, implying a standard deviation of a factor of 1·6 if the variation is normally distributed. Fig. 16(b) shows that 94% of the 194 calculated values of reference strain γ_r lie within a factor of 2 of the measured values, implying a standard deviation of a factor of 1·4. And Fig. 16(c) shows that all 280 calculated values of curvature parameter a effectively lie within a factor of 1·3 of the interpreted measurements.

The overall significance of the residual deviations in modulus reduction, G/G_0, between predictions and measurements can best be assessed by plotting predicted against measured values for all 3860 data points accumulated from all the tests, on those soils in the new database that are sufficiently well classified to enable the comparison. This is presented in Fig. 17, where it can be seen that 98% of predictions lie within a factor of 1·3 from the measurements. Assuming a standard distribution of error, this implies a standard deviation of a factor of 1·13 arising as an unresolved variability.

Figure 18 shows the degradation curves calculated using

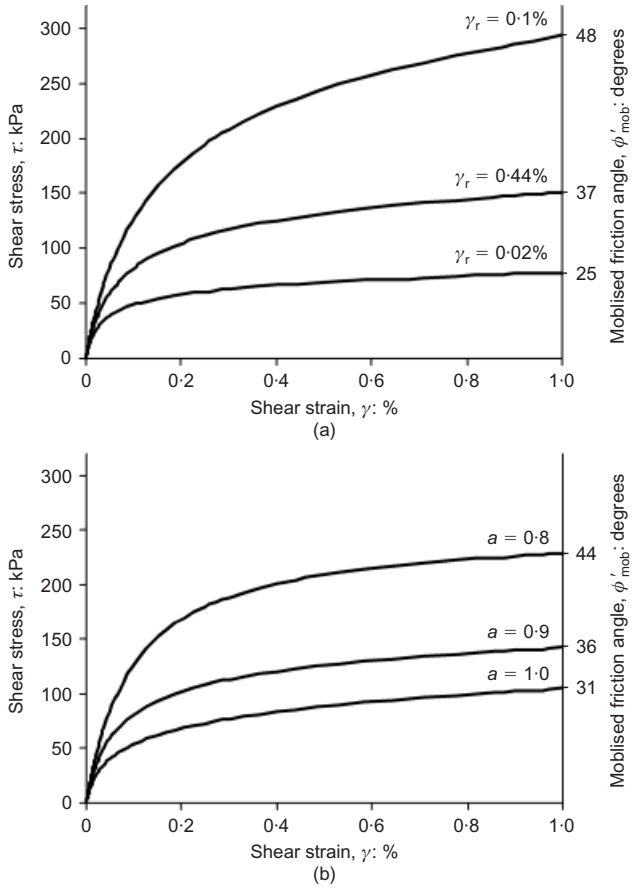

Fig. 15. Effect of γ_r and a on the shear stress–strain curve ($G_0 = 250$ MPa, $p' = 100$ kPa): (a) $a = 0{\cdot}88$; (b) $\gamma_r = 0{\cdot}044\%$

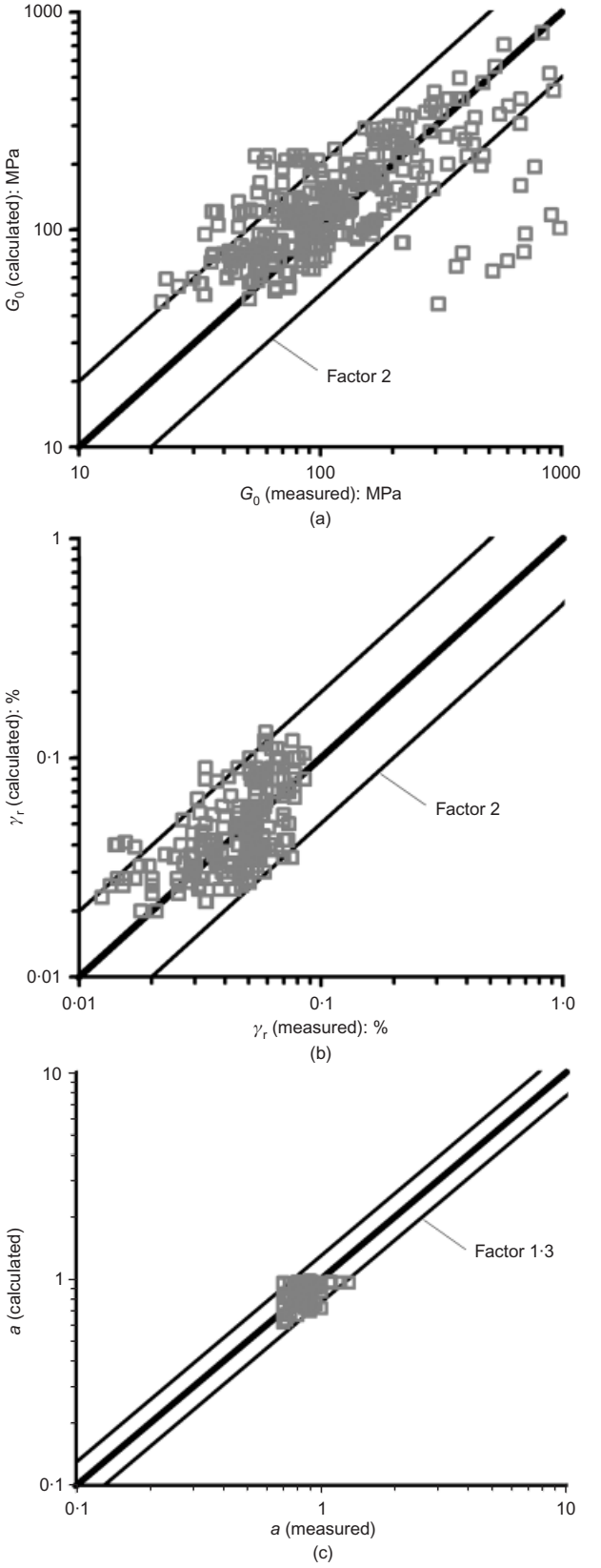

Fig. 16. Comparison of measured and calculated values of (a) G_0 (345 tests), (b) γ_r (194 tests) and (c) a (280 tests)

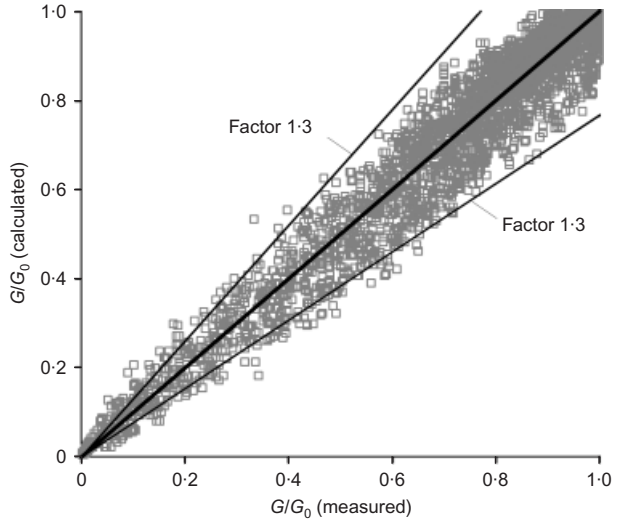

Fig. 17. Comparison of measured and calculated G/G_0 values (3860 data points)

equations (5), (11), (12) and (13) for ten named soils in clearly designated tests, compared with the corresponding raw test data. These ten examples are chosen to illustrate the full range of sandy soils having different void ratios, relative densities and uniformity coefficients. The whole range of the database and its central tendency are included in each case so that the success of the new predictive tools can be perceived.

APPLICATION

Statistical correlations such as those produced here find their application in a risk-based approach to design when calculations are to be based on elementary soil classification data, prior to a decision on whether or not to conduct more expensive and time-consuming field or laboratory tests. The aim of this paper has been to offer the designer clear guidelines from which the shear stiffness G of a typical sand can be estimated at any required magnitude of strain, and an understanding of the possible variability in that estimate. In that regard it is striking that the new database leaves a factor of uncertainty on elastic stiffness G_0 of 1·6 for one standard deviation, whereas the similar factor on G/G_0 is as small as 1·13. The elastic stiffness G_0 must be a function of soil fabric, and sensitive to anisotropy; this functionality can obviously have no correlation with disturbed soil properties such as classification parameters. Clearly, engineers should be encouraged to measure G_0 by seismic methods in the field, if possible. Appropriate use of down-hole and cross-hole logging will provide G_0 values pertinent to the required mode of ground deformation, accounting for anisotropy (Clayton, 2011).

Although the uncertainty in stiffness degradation has been reduced to a great extent in the current work, this is only applicable in practice if three key parameters can be estimated: void ratio e, relative density I_D, and uniformity coefficient U_c. Although the sand replacement test can be used to obtain a measurement of void ratio in situ, it can be carried out only on exposed benches of soil. The determination of void ratio in sands at depth is more difficult. However, estimates of each of the three key parameters can, in principle, be made from an SPT probe with a split sampler. Relative density can be estimated from the corrected blow count N_{60} and the vertical effective stress (σ'_{v0} in kPa) as

$$I_D \approx \left(\frac{N_{60}}{20 + 0{\cdot}2\sigma'_{v0}}\right)^{0{\cdot}5} \tag{14}$$

following authors such as Gibbs & Holtz (1979) and Skempton (1986). And since the split sampler provides a disturbed sample, this can be sieved for U_c, and also subjected to maximum and minimum density and specific gravity tests from which e_{max} and e_{min} can be found. Accordingly, the void ratio in situ can be estimated from the relative density. There is therefore no practical barrier to the use in practice of the stiffness relations provided here.

Equations (5), (11), (12) and (13), taken together with the in situ measurement of G_0 in the required mode of ground deformation, permit the engineer to estimate the in situ stress–strain curve of sands, and Fig. 4 allows that value to be corrected for future changes in mean effective stress, within statistical bounds. These expressions can also be used in non-linear numerical analyses, permitting them to be validated through field testing. For example, Oztoprak & Bolton (2011) demonstrate the use of this modified hyperbola in FLAC3D, to explore the fitting of self-boring pressuremeter tests in Thanet sand. An excellent match was obtained when appropriate secant values of the in situ angle of friction and angle of dilation were used for the fully plastic expansion phase, and when an allowance was made for initial disturbance affecting the lift-off pressure. Further discussion is also made of the potential impact of errors and ambiguities in the various values selected for the model. Further work to predict ground movements in sand in various applications is under way.

CONCLUSIONS

In order to assess the non-linear shear stiffness of sand, a database has been constructed including the secant shear modulus degradation curves of 454 tests from the literature.

A new shear modulus equation (equation (6)) was derived, with strain-dependent coefficients. Using this equation for the very-small-strain range ($\gamma = 0{\cdot}0001\%$), the maximum shear modulus G_0 can be estimated by equation (6) within a factor of 1·6 for one standard deviation.

A modified hyperbolic relationship was fitted to the collected database of secant shear modulus curves in the form of equation (5), featuring three curve-fitting parameters: elastic threshold strain γ_e, reference strain γ_r at $G/G_0 = 0{\cdot}5$, and curvature parameter a.

The use of equations (5) and (6) in sequence provided a statistical methodology for refining optimum functional relationships. Linear relations between the characteristic strains γ_e and γ_r and the mean effective stress p' offered the best fit to data from the most common range of confining pressure (70 kPa to 600 kPa): these were given in equations (11) and (12).

Sands with more disperse particle sizes begin to lose their linear elastic stiffness at a smaller strain than is the case with more uniform sands; this is in accord with micromechanical reasoning based on premature slip occurring between large and small particles due to strain incompatibility. It was suggested that the product eI_D, which has the effect of delaying the onset of intergranular sliding in equations (11) and (12), might stand as a surrogate for grain angularity, which increases interlocking; the influence of p' was thought to have the same origins.

The curvature parameter a was found to be related to uniformity coefficient through equation (13), such that more uniformly graded sands suffer faster deterioration of stiffness with strain once intergranular sliding is under way.

The new empirical expression for shear modulus reduction G/G_0 is shown to make predictions that are accurate within

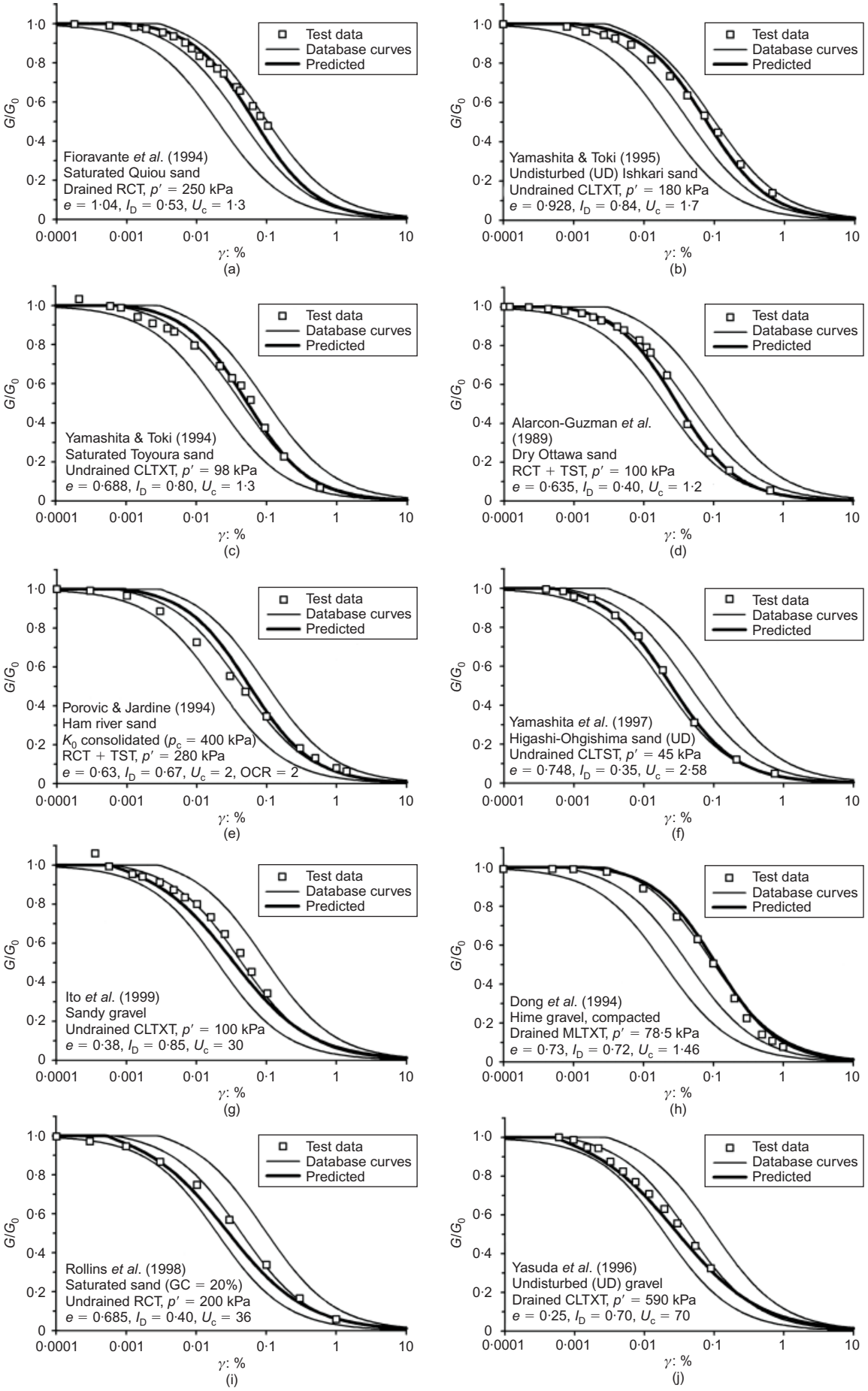

Fig. 18. Verification of predictions using equations (5), (11), (12) and (13) against shear modulus reduction curves of various sandy soils (UD, undisturbed; GC, gravel content)

a factor of 1·13 for one standard deviation of random error, as determined from 3860 data points. This very narrow spread applies irrespective of the test type and soil condition, within the range listed in Table 1. The initial elastic shear modulus, G_0, should always be measured if possible, but a new empirical relation is shown to provide estimates within a factor of 1·6 for one standard deviation of random error, as determined from 379 tests.

ACKNOWLEDGEMENTS

The work was supported by EPSRC Platform Grant GR/T18660/01. The first author was also supported by the Scientific Research Projects Coordination Unit of Istanbul University, Project No. YADOP-16527.

NOTATION

A	material constant
a	curvature parameter
B	material constant
c	scaling coefficient
D	diameter
D_{50}	average grain size
d	scaling coefficient
e	void ratio
e_g	empirical parameter in equation (1)
e_{max}	maximum void ratio
e_{min}	minimum void ratio
f	empirical parameter
G	secant shear modulus; shear stiffness
G_{max}	maximum shear modulus
G_0	initial elastic shear modulus
g	empirical parameter
I_D	relative density
m	material constant
N_{60}	corrected blow count
OCR	overconsolidation ratio
PI	plasticity index
p'	mean effective stress
p_a	reference (atmospheric) pressure
p_c	preconsolidation pressure
R^2	coefficient of determination
s'	effective stress
U_c	uniformity coefficient
V	$= 1 + e$
w	water content
γ	shear strain
γ_e	elastic threshold strain
γ_r	reference strain
σ'_{v0}	vertical effective stress
σ'_1	major effective principal stress
σ'_2	intermediate effective principal stress
σ'_3	minor effective principal stress
τ	shear stress
τ_{max}	maximum shear stress
ϕ'_{mob}	mobilised friction angle

REFERENCES

Alarcon-Guzman, A., Chameau, J. L., Leonards, G. A. & Frost, J. D. (1989). Shear modulus and cyclic undrained behavior of sands. *Soils Found*. **29**, No. 4, 105–119.

Arango, J. C. (2006). *Stress–strain behavior and dynamic properties of Cabo Rojo calcareous sands*. MSc thesis, University of Puerto Rico, San Juan, Puerto Rico.

Atkinson, J. H. (2000). Nonlinear soil stiffness in routine design. *Géotechnique* **50**, No. 5, 487–508, http://dx.doi.org/10.1680/geot.2000.50.5.487.

Atkinson, J. H. & Salfors, G. (1991). Experimental determination of stress–strain–time characteristics in laboratory and in situ tests. *Proc. 10th Eur. Conf. Soil Mech. Found. Engng, Florence* **3**, 915–956.

Cavallaro, A., Maugeri, M. & Ragusa, A. (2003). Small strain stiffness from in situ and laboratory tests for the city of Noto soil. In *Deformation characteristics of geomaterials* (eds H. Di Benedetto, T. Doanh, H. Geoffroy and C. Saizéat), pp. 267–274. Lisse, the Netherlands: Swets & Zeitlinger.

Charif, K. (1991). *Contribution à l'étude du comportement mécanique en petites et grandes déformation* ($\varepsilon > 10^{-6}$). PhD dissertation, Ecole Centrale Paris, France (in French).

Chegini, A. & Trenter, N. A. (1996). The shear strength and deformation behaviour of a glacial till. In *Advances in site investigation practice* (ed. C. Craig), pp. 851–866. London, UK: Thomas Telford.

Chung, R. M., Yokel, F. Y. & Drnevich, V. P. (1984). Evaluation of dynamic properties of sands by resonant column testing. *Geotech. Test. J.* **7**, No. 2, 60–69.

Clayton, C. R. I. (2011). Stiffness at small strain: research and practice. 50th Rankine Lecture. *Géotechnique* **61**, No. 1, 5–37, http://dx.doi.org/10.1680/geot.2011.61.1.5.

Darendeli, B. M. (2001). *Development of a new family of normalized modulus reduction and material damping curves*. PhD dissertation, University of Texas at Austin, TX, USA.

Delfosse-Ribay, E., Djeran-Maigre, I., Cabrillac, R. & Gouvenot, D. (2004). Shear modulus and damping ratio of grouted sand. *Soil Dynam. Earthquake Engng* **24**, No. 6, 461–471.

Dong, J., Nakamura, K., Tatsuoka, F. & Kohata, Y. (1994). Deformation characteristics of gravels in triaxial compression tests and cyclic triaxial tests. In *Pre-failure deformation of geomaterials* (eds S. Shibuya, T. Mitachi and S. Miura), pp. 17–23. Rotterdam, the Netherlands: Balkema.

D'Onofrio, A. & Penna, A. (2003). Small strain behaviour of a lime-treated silty sand. In *Deformation characteristics of geomaterials* (eds H. Di Benedetto, T. Doanh, H. Geoffroy and C. Saizéat), pp. 329–336. Lisse, the Netherlands: Swets & Zeitlinger.

Drnevich, V. P. & Richart, F. E. (1970). Dynamic prestraining of dry sand. *J. Soil Mech. Found. Div. ASCE* **96**, No. SM2, 453–469.

Ellis, E. A., Soga, K., Bransby, M. F. & Sato, M. (2000). Resonant column testing of sands with different viscosity pore fluids. *J. Geotech. Geoenviron. Engng* **126**, No. 1, 10–17.

Fahey, M. & Carter, J. P. (1993). A finite element study of the pressuremeter test in sand using a nonlinear elastic plastic model. *Can. Geotech. J.* **30**, No. 2, 348–362.

Fioravante, V., Jamiolkowski, M. & Lo Presti, D. C. F. (1994). Stiffness of carbonatic Quiou sand. *Proc. 8th Int. Conf. Soil Mech. Found. Engng, New Delhi* **1**, 163–168.

Gibbs, H. J. & Holtz, W. G. (1979). Discussion of 'SPT and relative density in coarse sands', by Marcuson and Bieganousky. *J. Geotech. Engng ASCE* **105**, No. GT3, 439–441.

Goddard, J. D. (1990). Nonlinear elasticity and pressure-dependent wave speeds in granular media. *Proc. R. Soc. Math. Phys. Sci*. **430**, No. 1878, 105–131.

Goto, S., Syamoto, Y. & Tamaoki, K. (1987). Dynamic properties of undisturbed gravel samples obtained by the in-situ freezing method. *Proc. 8th Asian Regional Conf. on Soil Mech. Found. Engng, Kyoto* **1**, 233–236.

Goto, S., Suzuki, Y., Nishio, S. & Hiroshi, O.-O. (1992). Mechanical properties of undisturbed Tone-River gravel obtained by in-situ freezing method. *Soils Found*. **32**, No. 3, 15–25.

Hardin, B. O. & Black, W. L. (1966). Sand stiffness under various triaxial stresses. *J. Soil Mech. Found. Div. ASCE* **92**, No. SM2, 667–692.

Hardin, B. O. & Drnevich, V. P. (1972a). Shear modulus and damping in soils: measurement and parameter effects. *J. Soil Mech. Found. Div. ASCE* **98**, No. SM6, 603–624.

Hardin, B. O. & Drnevich, V. P. (1972b). Shear modulus and damping in soils: design equations and curves. *J. Geotech. Engng* **98**, No. 7, 667–692.

Hardin, B. O. & Kalinski, M. E. (2005). Estimating the shear modulus of gravelly soils. *J. Geotech. Geoenviron. Engng* **131**, No. 7, 867–875.

Hashiba, T. (1971). Simple shear apparatus using an inclinometer. *Soils Found*. **11**, No. 3, 113–119.

Hatanaka, M. & Uchida, A. (1995). Effect of test methods on the cyclic deformation characteristics of high quality undisturbed gravel samples. In *Static and dynamic properties of gravelly soils* (eds M. D. Evans and R. J. Fragaszy), Geotechnical Special Publication No. 56, pp. 136–161. Reston, VA, USA: ASCE.

Hatanaka, M., Suzuki, Y., Kawasaki, T. & Endo, M. (1988). Cyclic undrained shear properties of high quality undisturbed Tokyo gravel. *Soils Found*. **28**, No. 4, 57–68.

Ishihara, K. (1996). *Soil behaviour in earthquake geotechnics*. Oxford, UK: Oxford University Press.

Ito, K., Goto, Y., Ishihara, K., Yasuda, S. & Yoshida, N. (1999). Detailed in-situ and laboratory tests on the improved ground in Port Island. *Proc. 2nd Int. Conf. on Earthquake Geotech. Engng, Lisboa*, 47–52.

Iwasaki, T. & Tatsuoka, F. (1977). Effects of grain size and grading on dynamic shear moduli of sands. *Soils Found*. **17**, No. 3, 19–35.

Iwasaki, T., Tatsuoka, F. & Takagi, Y. (1978). Shear moduli of sands under cyclic torsional shear loading. *Soils Found*. **18**, No. 1, 39–50.

Jardine, R. J., Potts, D. M., Fourie, A. B. & Burland, J. B. (1986). Studies of the influence of non-linear stress–strain characteristics in soil-structure interaction. *Géotechnique* **36**, No. 3, 377–396, http://dx.doi.org/10.1680/geot.1986.36.3.377.

Jardine, R. J., Kuwano, R., Zdravkovic, L. & Thornton, C. (2001). Some fundamental aspects of the pre-failure behaviour of granular soils. *Proc. 2nd Int. Symp. on Pre-failure Deformation Characteristics of Geomaterials, Torino*, 1077–1111.

Jovicic, V. & Coop, M. R. (1997). Stiffness of coarse-grained soils at small strains. *Géotechnique* **47**, No. 3, 545–561, http://dx.doi.org/10.1680/geot.1997.47.3.545.

Katayama, I., Fukui, F., Satoh, M., Makihara, Y. & Tokimatsu, K. (1986). Comparison of dynamic soil properties between undisturbed and disturbed dense sand samples. *Proc. 21st Ann. Conv. Japan. Soc. Soil Mech. Found. Engng, Sapporo*, 583–584 (in Japanese).

Koga, Y., Matsuo, O. & Sugawara, N. (1994). In-situ measurement of shear moduli of soils and its evaluation. In *Pre-failure deformation of geomaterials* (eds S. Shibuya, T. Mitachi and S. Miura), pp. 213–216. Rotterdam, the Netherlands: Balkema,

Kokusho, T. (1980). Cyclic triaxial test of dynamic soil properties for wide strain range. *Soils Found*. **20**, No. 2, 45–60.

Kokusho, T. & Esashi, Y. (1981). Cyclic triaxial test on sands and coarse materials. *Proc. 10th Int. Conf. Soil Mech. Found. Engng, Stockholm* **1**, 673–676.

Kokusho, T. & Tanaka, Y. (1994). Dynamic properties of gravel layers investigated by in-situ freezing sampling. In *Ground failure under seismic conditions* (eds S. Prakash and P. Dakoulas), Geotechnical Special Publication No. 44, pp. 121–140. Reston, VA, USA: ASCE.

Laird, J. P. & Stokoe, K. H. (1993). *Dynamic properties of remolded and undisturbed soil samples tested at high confining pressures*, Geotech. Engrg. Rep. GR93–6. Palo Alto, CA, USA: Electrical Power Research Institute.

Lanzo, G., Vucetic, M. & Doroudian, M. (1997). Reduction of shear modulus at small strains in simple shear. *J. Geotech. Geoenviron. Engng* **123**, No. 11, 1035–1042.

Lo Presti, D. C. F., Jamiolkowski, M., Pallara, O., Cavallaro, A. & Pedroni, S. (1997). Shear modulus and damping of soils. *Géotechnique* **47**, No. 3, 603–617, http://dx.doi.org/10.1680/geot.1997.47.3.603.

Mair, R. J. (1993). Developments in geotechnical engineering research: application to tunnels and deep excavations. Unwin Memorial Lecture 1992. *Proc. Instn Civil Engrs Civ. Engng* **97**, No. 1, 27–41.

Maher, M. H., Ro, K. S. & Welsh, J. P. (1994). High strain dynamic modulus and damping of chemically grouted sand. *Soil Dynam. Earthquake Engng* **13**, No. 1, 131–138.

McDowell, G. R. & Bolton, M. D. (1999). A micro mechanical model for isotropic cyclic loading of isotropically clastically compressed soil. *Granular Matter* **1**, No. 4, 183–194.

Menq, F. Y. (2003). *Dynamic properties of sandy and gravelly soils*. PhD dissertation, University of Texas at Austin, TX, USA.

Menq, F. Y. & Stokoe, K. H. (2003). Linear dynamic properties of sandy and gravelly soils from large-scale resonant tests. In *Deformation characteristics of geomaterials* (eds H. Di Benedetto, H. Geoffroy, T. Doanh and C. Sauzéat), pp. 63–71. Lisse, the Netherlands: Swets & Zeitlinger.

Ogata, N. & Yasuda, M. (1982). Dynamic properties of undisturbed samples containing gravels. *Proc. 17th Japan. Nat. Conf. Soil Mech. Found. Engng, Okinawa* **1**, 1609–1612 (in Japanese).

Oztoprak, S. & Bolton, M. D. (2011). Parameter calibration of a modified hyperbolic model for sands using pressuremeter test data. *Proc. 5th Int. Symp. on Deformation Characteristics of Geomaterials, Seoul*, 949–956.

Park, C.-S. (1993). *Deformation and strength characteristics of a variety of sands by plane strain compression tests*. DEng thesis, University of Tokyo, Japan (in Japanese).

Porovic, E. & Jardine, R. J. (1994). Some observations on the static and dynamic shear stiffness of Ham River sand. *Proc. 1st Int. Symp. on Pre-failure Deformation of Geomaterials, Sapporo* **1**, 25–30.

Roesler, S. K. (1979). Anisotropic shear modulus due to stress anisotropy. *J. Geotech. Engng Div. ASCE* **105**, No. 7, 871–880.

Rollins, K. M., Evans, M. D., Diehl, N. B. & Daily, W. D. (1998). Shear modulus and damping relationships for gravels. *J. Geotech. Geoenviron. Engng* **124**, No. 5, 396–405.

Saxena, S. K., Avramidis, A. S. & Reddy, K. R. (1988). Dynamic moduli and damping ratios for cemented sands at low strains. *Can. Geotech. J.* **25**, No. 2, 353–368.

Seed, H. B. & Idriss, I. M. (1970). *Soil moduli and damping factors for dynamic response analyses*, Report EERC 70–10. Berkeley, CA, USA: University of California.

Seed, H. B., Wong, R. T., Idriss, I. M. & Tokimatsu, K. (1986). Moduli and damping factors for dynamic analyses of cohesionless soil. *J. Geotech. Engng* **112**, No. GT11, 1016–1032.

Shibuya, S., Mitachi, T., Yamashita, S. & Tanaka, H. (1996). Recent Japanese practice for investigating elastic stiffness of ground. In *Advances in site investigation practice* (ed. C. Craig), pp. 875–886. London, UK: Thomas Telford.

Silver, M. L. & Seed, H. B. (1971). Deformation characteristics of sands under cyclic loading. *J. Soil Mech. Found. Div. ASCE* **97**, No. SM8, 1081–1098.

Simpson, B. (1992). Retaining structures: displacement and design. *Géotechnique* **42**, No. 4, 541–576, http://dx.doi.org/10.1680/geot.1992.42.4.541.

Skempton, A. W. (1986). Standard penetration test procedures and the effects in sands of overburden pressure, relative density, particle size, ageing and overconsolidation. *Géotechnique* **36**, No. 3, 425–447, http://dx.doi.org/10.1680/geot.1986.36.3.425.

Stokoe, K. H., Hwang, S. K., Lee, J. N. K. & Andrus, R. D. (1994). Effects of various parameters on the stiffness and damping of soils at small to medium strains. *Proc. 1st Int. Symp. on Pre-failure Deformation of Geomaterials, Sapporo* **2**, 785–816.

Stokoe, K. H., Darendeli, M. B., Andrus, R. D. & Brown, L. T. (1999). Dynamic soil properties: laboratory, field and correction studies. *Proc. 2nd Int. Conf. on Earthquake Geotech. Engng, Lisbon* **3**, 811–845.

Tanaka, Y., Kudo, Y., Yoshida, Y. & Ikemi, M. A. (1987). *Study on the mechanical properties of sandy gravel-dynamic properties of reconstituted sample*, Report U87019. Tokyo, Japan: Central Research Institute of Electric Power Industry.

Tatsuoka, F. & Shibuya, S. (1991). Deformation characteristics of soils and rocks from field and laboratory tests. *Proc. 9th Asian Regional Conf. on Soil Mech. and Found. Engng, Bangkok* **2**, 101–170.

Teachavorasinskun, S., Shibuya, S. & Tatsuoka, F. (1991). Stiffness of sands in monotonic and cyclic loading in simple shear. *Proceedings of the ASCE Geotechnical Engineering Congress*, Boulder, CO. Geotechnical Special Publication No. 27, Vol. 1, pp. 863–878. Reston, VA, USA: ASCE.

Teachavorasinskun, S., Tatsuoka, F., Kenkyo, K. & Yasuhara, K. (1992). Effect of cyclic prestraining on the liquefaction strength of sand. *Proceedings of the conference on behaviour of offshore structures*, London, pp. 1345–1356.

Tika, T., Kallioglou, P. & Pitilakis, K. (1999). Laboratory measurement of dynamic properties of natural soils. *Proc. 2nd Int. Symp. on Pre-failure Deformation Characteristics of Geomaterials, Torino* **1**, 239–244.

Tika, T., Kallioglou, P., Papadopoulou, A. & Pitilakis, K. (2003). Shear modulus and damping of natural sands. In *Deformation characteristics of geomaterials* (eds H. Di Benedetto, H. Geoffroy, T. Doanh and C. Sauzéat), pp. 401–407. Lisse, the Netherlands: Swets & Zeitlinger.

Tokimatsu, K. & Hosaka, Y. (1986). Effects of sample disturbance on dynamic properties of sand. *Soils Found*. **26**, No. 1, 53–64.

Tokimatsu, K., Yamazaki, T. & Yoshimi, Y. (1986). Soil liquefaction evaluations by elastic shear moduli. *Soils Found*. **26**, No. 1, 25–35.

Vinale, F., d'Onofrio, A., Mancuso, C. & Santucci de Magistris, F. (1999). The pre-failure behaviour of soils as construction materials. *Proc. 2nd Int. Symp. on Pre-failure Deformation Characteristics of Geomaterials, Torino* **2**, 955–1003.

Yamashita, S. & Suzuki, T. (1999). Young's and shear moduli under different principal stress directions of sand. *Proc. 2nd Int. Symp. on Pre-failure Deformation Characteristics of Geomaterials, Torino* **1**, 149–158.

Yamashita, S. & Toki, S. (1994). Cyclic deformation characteristics of sands in triaxial and torsional tests. *Proc. 1st Int. Symp. on Pre-failure Deformation of Geomaterials, Sapporo* **1**, 31–360.

Yamashita, S., Shibuya, S. & Tanaka, H. (1997). A case study for characterizing undrained cyclic deformation properties in young sand deposit from in-situ and laboratory tests. *Soils Found*. **37**, No. 2, 117–126.

Yang, B. E. (2007). *Shear strength modeling of cemented sand*, Master thesis, University of Notre Dame, Indiana, USA.

Yasuda, N. (1992). Behavior of embankment dams during earthquakes and dynamic deformation characteristics of rockfill materials. *Journal Japan Soc. Dam Engs*, No. 6, 43–59 (in Japanese).

Yasuda, N. & Matsumoto, N. (1993). Dynamic deformation characteristics of sands and rockfill materials. *Can. Geotech. J.* **30**, No. 5, 747–0757.

Yasuda, N. & Matsumoto, N. (1994). Comparisons of deformation characteristics of rockfill materials using monotonic and cyclic loading laboratory tests and in situ tests. *Can. Geotech. J.* **31**, No. 2, 162–174.

Yasuda, N., Ohta, N. & Nakamura, A. (1996). Dynamic deformation characteristics of undisturbed riverbed gravels. *Can. Geotech. J.* **33**, No. 2, 237–249.